# 18. THE DISTRIBUTION OF HII REGIONS

P. G. MEZGER

*National Radio Astronomy Observatory*, Green Bank, W. Va., U.S.A., and Max-Planck-Institut für Radioastronomie, Bonn, Germany*

**Abstract.** The distribution of optically observed HII regions and OB stars with galactic longitude indicates that it is primarily determined by extinction by interstellar dust. Thus optical observations can, at the best, reveal the local structure in the vicinity of the sun. Radio observations, on the other hand, are not affected by dust. Thus the distribution of galactic radio sources, which peaks in the northern part at about $l^{II} = 17°.5$, must be related to the large-scale structure of our Galaxy. Two radio recombination line surveys of the northern and southern sky yield kinematic distances. If only the 'giant HII regions' are retained, the following distribution is obtained: (1) Only 5 giant HII regions are found within the 4 kpc arm. (2) The bulk of the giant HII regions is concentrated in a ring between 4 and 6 kpc from the galactic center. (3) There are other concentrations of giant HII regions indicating the existence of the Sagittarius and Perseus arm. (4) The three features revealed by optical observations of HII regions in the vicinity of the sun cannot be matched with the large-scale distribution outlined by giant HII regions. This is particularly true for the so-called Orion arm. (5) At distances beyond 13 kpc from the galactic center virtually no giant HII regions are found. (6) The surface density of giant HII regions attains its maximum between 4 and 8 kpc; the surface density of neutral hydrogen (HI) attains its maximum between 11 and 15 kpc, but the actual space density of HI in the region 4 to 8 kpc may still be rather high.

## 1. Spiral Arms and Star Formation

Spiral arms in our galaxy appear to be defined primarily by a density of the interstellar matter higher than that in the interarm region and by the existence of hot, massive early-type stars which ionize the surrounding gas. According to a theory advanced by Lin and Shu (1964, 1966), the spiral pattern is maintained by a density wave which rotates between 4 and 12 kpc from the galactic center with an angular velocity lower than that of the general galactic rotation of the Population I material. As the interstellar material passes through the density wave potential minimum, it is compressed and star formation on a large scale – as observed in external galaxies – may thus be initiated. It was first suggested by Clark (1965) and subsequently confirmed by various authors (for a comprehensive review see Mebold, 1969) that the interstellar matter in spiral arms consists of dense, cool clouds embedded in (and possibly in pressure equilibrium with) an intercloud gas with temperatures of several thousand degrees K. It may well be that O-star clusters and associations form out of these dense and cool clouds.

## 2. Star Formation and HII Regions

The radio flux from an ionization bounded HII region is directly related to the flux of Lyman continuum photons from the exciting star(s). It is found that most of the

* The NRAO is operated by Associated Universities, Inc., under contract with the National Science Foundation.

*Becker and Contopoulos (eds.), The Spiral Structure of Our Galaxy*, 107–121. 

H II regions observed as thermal radio sources require one or more early-type O-stars for their ionization, i.e. stars with main sequence lifetimes of a few $10^6$ years. My associates and I have investigated in some detail the obvious relation between H II regions and regions of star formation in a number of papers, which are summarized in a recent review paper (Mezger, 1969) or which are in preparation (Felli and Churchwell, 1969), respectively. In the context of the present review paper on galactic structure the following results are relevant:

(a) Most H II regions which are strong thermal radio sources consist of one or more compact components of high electron density but small linear dimensions, which are embedded in an extended low-density H II region. It appears that the compact H II regions represent very early evolutionary stages of subgroups, which Blaauw (1964) observes in O-star associations (Schraml and Mezger, 1969).

(b) These compact components, even in nearby extended H II regions, are often heavily obscured by dust. As a rule, their exciting stars cannot be seen (Schraml and Mezger, 1969).

(c) On the other hand, most of the optically observed H II regions (e.g. those catalogued by Sharpless, 1959) are only weak thermal radio sources. It appears that they represent later evolutionary stages, where the ionized gas has expanded and the circumstellar dust clouds of the exciting stars have been dispersed or destroyed (Felli and Churchwell, 1969).

It is well known that, owing to the extinction by interstellar dust, optical observations of H II regions and their exciting stars are generally limited to distances $\lesssim 3$ kpc from the sun while radio waves are hardly affected by the interstellar medium. However, in comparing the spiral structure of our galaxy as outlined by optical and radio observations of H II regions the additional selection effect that radio and optical observations pertain to different evolutionary stages of H II regions and O-star clusters should be considered, too.

## 3. Optical Observations of H II Regions

Rather than reviewing all the earlier optical work pertaining to H II regions and spiral structure I will refer in this section to what appears to be the most complete set of observations of OB-stars and H II regions.

Miss Sim (1968), based on the Hamburg-Warner and Swasey survey, investigated the distribution of $OB^+$, OB and $OB^-$-stars as a function of both galactic longitude (1968) and latitude (private communication). The former results are reproduced in Figure 1a–c. Using the catalog of H II regions by Sharpless (1959) I have prepared the corresponding diagram for the longitude distribution of optically visible H II regions* in Figure 1d. The correlation between H II regions and early-type stars is best for the $OB^+$-stars. In latitude, the half power width of the Sharpless H II regions is about 3°, that of the OB-stars is between 4° and 5° (Sim, private communication).

* The percentage of H II regions in Figure 1d refers to the total number of 224 H II regions in the longitude range $0° \leqslant l^{II} \leqslant 180°$.

https://doi.org/10.1017/S0074180900000383 Published online by Cambridge University Press

The distribution of both OB-stars and H II regions exhibits a minimum between $20° < l^{II} < 90°$, with the exception of the Cygnus X region ($l^{II} \simeq 76°$). As will be shown later, it is, however, that very longitude range which coincides with the most active regions of star formation in our galaxy. Obviously, obscuration by dust clouds is the predominant factor that determines the distributions of OB-stars and H II regions in Figure 1a–d.

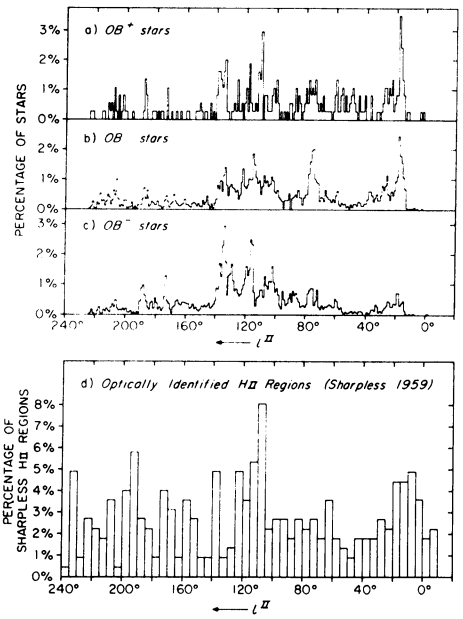


Fig. 1 (a)-(c). Distribution of OB-stars in galactic longitude. – (d) Distribution of optically visible H II regions in galactic longitude.

Courtès *et al.* (1968) investigated the local distribution of H II regions, using both photometric distances of exciting stars and kinematic distances derived from optically determined radial velocities. Figure 2, reproduced from their paper, shows the distribution of H II regions based on photometric distances. There appear reasonably well outlined parts of the Perseus, Orion, and Sagittarius arm. At a longitude of 330° three distant H II regions are seen which are probably members of the Norma-Scutum arm. The pitch angle of the three arms is about 20°.

## 4. Radio Continuum Surveys

The era of high resolution surveys of the galactic continuum radiation in the GHz range was opened with a present-day classic paper by Westerhout (1958). In this frequency range the thermal radiation from ionized hydrogen begins to predominate over the diffuse non-thermal background radiation. Westerhout discovered three basic characteristics of the galactic continuum radiation:

https://doi.org/10.1017/S0074180900000383 Published online by Cambridge University Press

(1) The bulk of the galactic continuum radiation comes from a narrow range centered about the galactic plane (referred to as disk component). It consists of a thermal component with a very narrow distribution in latitude (HPW $\simeq 1.^{\circ}6$) and a non-thermal disk component with a considerably wider HPW of $\simeq 4.^{\circ}2$.

(2) As a function of galactic longitude the thermal component attains a maximum at $l^{II} \simeq 26^{\circ}$, whereas the non-thermal component increases steadily towards the galactic center. From this latter result Westerhout concluded that most of the ionized hydrogen must be concentrated in a ring just outside the 4 kpc arm.

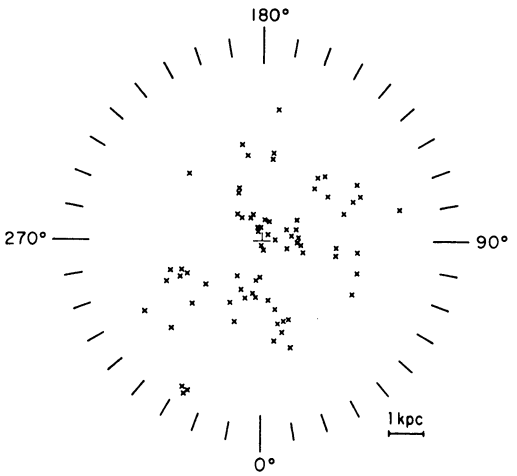


Fig. 2. Projected positions of optically visible HII regions, based on photometric distances of their exciting stars.

(3) Superimposed on the disk components are a number of discrete sources compiled in the Westerhout catalog; these are presently referred to by their W-numbers.

Subsequent surveys have refined Westerhout's observations (e.g. Altenhoff *et al.*, 1960) or expanded them to the southern part of our galaxy (e.g. Mathewson *et al.*, 1962) but did not essentially change Westerhout's basic conclusions.

It took exactly 10 years before another big step forward was made in the radio continuum surveys of our galaxy. Stimulated by the detection of radio recombination lines (following section) and a limited survey at 5 GHz with the NRAO 140-ft telescope (Mezger and Henderson, 1967) Altenhoff, using the NRAO 140-ft telescope at 2.7 GHz carried out a complete survey of the galactic plane visible from Green Bank within the latitude limits $b^{II} = \pm 2^{\circ}$. A first report on his results was published in 1968. Owing to both the higher angular resolution of the 140-ft telescope and the higher sensitivity of modern broadband radiometers equipped with low-noise preamplifiers, Altenhoff has detected about ten times as many sources as given in Westerhout's source catalog. It turned out that in Altenhoff's survey Westerhout's thermal disk

component is nearly completely resolved into individual thermal sources*. In Table I recent high resolution continuum surveys of the northern and southern part of the Galaxy are listed.

In the remainder of this section I will refer mainly to three northern surveys by Altenhoff *et al.* (1969). These surveys were made with telescopes of different sizes; owing to an appropriate frequency selection (Table I) between 1.4 and 5 GHz, the angular resolution of the three surveys was nearly identical, i.e. $\simeq 10'$. The same reduction method was applied, including the separation between sources and background.

This procedure yielded another new and important characteristic of galactic sources. Their spectra could now be determined from the peak flux densities (or main beam brightness temperatures, respectively) at the three frequencies without any additional assumptions on the source size which make earlier work on galactic spectra so highly unreliable. Altenhoff *et al.* (1969) determined spectra of 206 galactic sources out of which 141 have spectral indices ($S \propto \nu^{\alpha}$) $\alpha \gtrsim -0.3$ and therefore could be thermal. An unexpectedly large fraction (31%) of the investigated sources have spectral indices $\alpha \lesssim -0.3$ and thus are obviously non-thermal. Altenhoff (1968) could not find a strong correlation between the distribution of these non-thermal sources and the diffuse non-thermal background radiation. However, at least in some cases non-thermal sources appear to be closely associated with HII regions (e.g. W 28, W 49, W 51).

Figure 3 shows the longitudinal distribution of sources. All three surveys have in common the longitude range $12° \leqslant l^{II} \leqslant 55°$. The two surveys at 2.7 and 5 GHz cover the additional range $345° \rightarrow 0° \rightarrow 12°$. Only the 2.7 GHz survey extends beyond 55°; that part of the reduction is preliminary and the results are therefore indicated by dashed lines. (The hatched areas pertain to the 5 GHz H 109α and continuum survey of northern sources which will be discussed in the following section.)

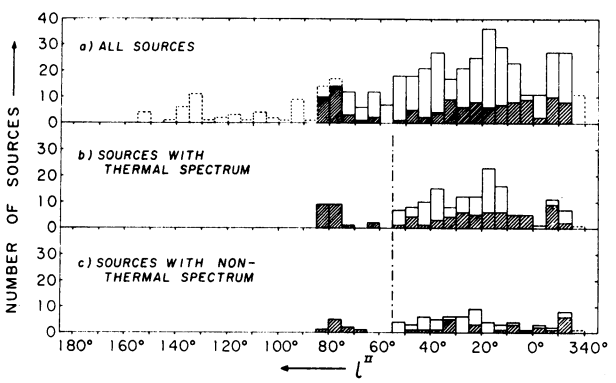


Fig. 3 (a)–(c). Distribution of galactic radio sources in galactic longitude, as observed at $\nu = 2.7$ GHz. The shaded areas pertain to the H 109α observations at $\nu = 5$ GHz.

* From this result it cannot be implied, however, that most of the ionized hydrogen in our galaxy is concentrated in completely ionized HII regions since radio radiation depends on the emission measure, i.e. the square of the electron density integrated along the line of sight. Thus radio surveys are heavily weighted towards regions of hot, dense plasma.

https://doi.org/10.1017/S0074180900000383 Published online by Cambridge University Press

TABLE I

Recent high resolution galactic continuum surveys

| $\nu$/MHz | Telescope | HPBW | Detection limit (peak flux density) | $l^{II}$ | $b^{II}$ | Completeness | References |
|---|---|---|---|---|---|---|---|
| 408 | Mills cross | 2′.8 in EW | | 210°–0°<br>0°–50° | | 72 selected regions | (1) |
| 1420 | NRAO 300-ft. telescope | 10′.2 | 0.5 f.u. | 12°–55° | ± 5° | | (2) |
| 1420 | Parkes 210-ft. telescope | 14′. | | 280°–355° | ± 2° | | (3) |
| 2700 | NRAO 140-ft. telescope | 11′.0 | 2.0 f.u. | 345°–0°<br>0°–155° | ± 2° | | (2) |
| 2700 | Parkes 210-ft. telescope | 7′.3 | 1.0 f.u. | 288°–0°<br>0°–38° | ± 2° | | (4) |
| 5000 | NRAO 140-ft. telescope | 6′.5 | | 347°–0°<br>0°–210° | | 120 individual sources | (5) |
| 5000 | Parkes 210-ft. telescope | 4′.0 | | 210°–0°<br>0°–50° | | 63 selected regions | (6) |
| 5000 | Fort Davis 85-ft. telescope | 10′.8 | 3.0 f.u. | 340°–0°<br>0°–55° | ± 3° | | (2) |
| 15375 | NRAO 140-ft. telescope | 2′.0 | | 350°–0°<br>0°–210° | | 22 selected regions | (7) |

(1) Shaver and Goss (1969); (2) Altenhoff *et al.* (1969); (3) Hill (1968); (4) Staff of CSIRO, Div. of Radiophys. (1969); (5) Reifenstein *et al.* (1970); (6) Goss and Shaver (1969); (7) Schraml and Mezger (1969).

https://doi.org/10.1017/S0074180900000383 Published online by Cambridge University Press

Part (a) of Figure 3 shows the distribution of all sources observed at 2.7 GHz. Parts (b) and (c) are the corresponding distributions of thermal and non-thermal sources. Note that the sum of thermal and non-thermal sources for a given longitude interval is usually smaller than the total number of all sources observed at 2.7 GHz. The larger fraction of sources are H II regions and it appears to be permissible, therefore, to compare the general source distribution in Figure 3a with that of optically identified H II regions in Figure 1d. The difference in the two distributions is evident and there appears to be – in the large-scale distribution at least – an anticorrelation rather than a correlation. The distribution of radio sources exhibits a minimum about the galactic center, increases rapidly to a maximum about 17.5° and gradually tapers off towards the galactic anticenter which is an obvious 'zone of avoidance' of radio sources. There are secondary maxima in the source distribution about 37.5°, (62.5°), 77.5°, (92.5°), 132.5° and 152.5°. The secondary maxima whose longitudes are given in brackets hinge on an increased source number in one longitude interval only and statistical fluctuations therefore cannot be excluded completely. It is of interest to note, however, that only these somewhat uncertain maxima in the source distribution are matched by corresponding maxima in the optical distribution (Figure 1d).

This obvious anticorrelation in the distribution of optically identified H II regions and radio sources appears to be the joint result of two selection effects discussed in Section 2 (radio observations favor O-star associations and clusters in very early evolutionary stages) and Section 3 (obscuration by dust especially in regions of active star formation). It is thus clear that only radio observations can further the investigation of the large-scale spiral structure of our galaxy.

The latitude distribution of radio sources and optically identified H II regions given in Figure 4a–d tends to confirm this conclusion. The distribution of radio sources is obviously the result of the superposition of a narrow distribution representing the intrinsically intense, distant sources and a much wider distribution representing nearby and intrinsically weak sources. The optically identified H II regions show only the wide distribution representing the local objects.

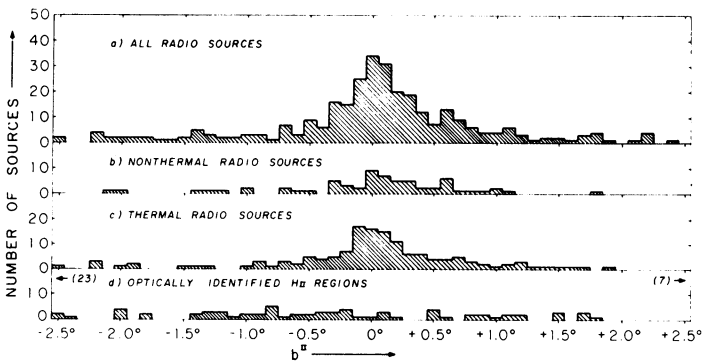


Fig. 4 (a)–(c). Distribution of galactic radio sources in galactic latitude as observed at $\nu = 2.7$ GHz. – (d) Distribution of optically visible H II regions in galactic latitude.

https://doi.org/10.1017/S0074180900000383 Published online by Cambridge University Press

It is of interest to note that the non-thermal sources have a smoother distribution in longitude (Figure 3c) and a wider distribution in latitude (Figure 4b) as compared to the thermal radio sources. They may represent a distribution of objects somewhere between the very distant 'giant H II regions' and the intrinsically weak H II regions.

The large fraction of non-thermal sources with relatively high surface brightness and small angular dimensions is still a puzzle and can hardly be explained by an average birth rate of one supernova per hundred years.

## 5. Radio Recombination Line Surveys

It was a tantalizing fact for observers of the galactic continuum emission to know that they could observe H II regions at the opposite side of our galaxy but at the same time to know that there was no way to determine their distances. This was one of the main incentives for us to search for radio recombination lines which could provide us with radial velocities and hence kinematic distances of H II regions. Three limited recombination line surveys (Mezger and Höglund, 1967; Dieter, 1967; McGee and Gardner, 1968) followed the first unambiguous and quantitative observation of the H 109α-line by Höglund and Mezger (1965). Subsequently, these surveys were rendered obsolete by two rather complete H 109α line surveys of the northern and southern galaxy. Data pertinent to these two surveys are given in Table II.

Owing to some overlap in the two surveys the total number of radial velocities of individual H II regions is 201 rather than the sum of the two numbers in the sixth column, 213. Selection criterion for sources to be included in the two surveys was a value of the peak antenna temperature of $T_c \geqslant 1$ K. We feel, however, that some sources in the range $1.3\,\mathrm{K} \geqslant T_c \geqslant 1\,\mathrm{K}$ may have been missed. The distribution of all sources included in the two surveys is shown in Figure 5a. Owing to the different characteristics

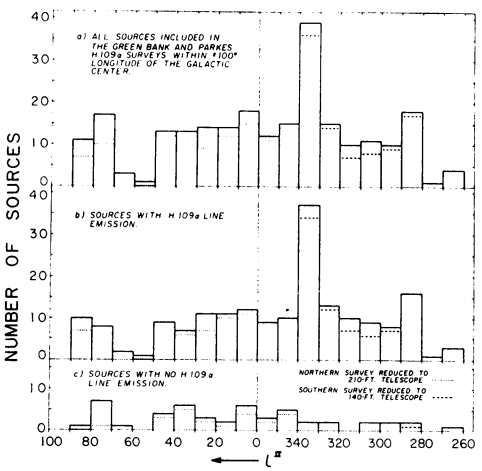


Fig. 5 (a)–(c). Distribution of radio sources included in northern and southern H 109α surveys. Dashed and dotted line refers to distributions reduced for instrumental selection effects (see text).

https://doi.org/10.1017/S0074180900000383 Published online by Cambridge University Press

TABLE II

The NRAO-MIT and NRAO-CSIRO-MIT H 109α surveys of northern and southern galactic sources

| Telescope | HPBW | $\eta_B$ | $T_c$ (min) | $S_5$ (min) | Total number of sources | Sources with H 109α emission | | Sources without H 109α emission | | References |
|---|---|---|---|---|---|---|---|---|---|---|
| | | | | | | Number | % | Number | % | |
| NRAO 140-ft. | 6′.5 | 0.7 | 1 0 | 3.8 | 120 | 82 | 68 | 38 | 32 | (1) |
| Parkes 210-ft. | 4′.0 | 0.45 | 1.0 | 2.6 | 151 | 131 | 87 | 20 | 13 | (2) |

(1) Reifenstein *et al.* (1970); (2) Wilson *et al.* (1970).



https://doi.org/10.1017/S0074180900000383 Published online by Cambridge University Press

of the two telescopes (see first three columns of Table II) the Parkes 210-ft telescope is more sensitive to point sources but less sensitive to extended sources than the NRAO 140-ft telescope. The dashed and dotted lines in Figure 5 represent the southern survey if observed with the 140-ft telescope and the northern survey if observed with the 210-ft telescope, respectively. However, the thus corrected source distributions have to be viewed with caution, since we can only estimate those sources which would have been rejected but not those which would have been added to either survey.

Figures 5a, b show the distribution of observed sources with and without H 109α emission, respectively. Sources with line emission are considered to be thermal, those without line emission, non-thermal. The source distributions Figures 5a–c in the longitude interval 345° through 0° to 85° are given in Figure 3 as shaded areas. It is of interest to note that for the northern part of our galaxy the percentage of sources without H 109α emission (32%) is nearly the same as the percentage of non-thermal sources (31%) identified on grounds of their continuum spectral indices (Section 4), thus confirming the unexpectedly high fraction of non-thermal sources. For the southern part the fraction of sources with no H 109α emission (13%) is considerably lower. This surprising result has yet to be confirmed by an investigation of the continuum spectra of southern sources.

Radial velocities of H II regions were obtained from their recombination line emission with a typical accuracy of $\pm 1$ km $s^{-1}$. Kinematic distances were derived using the Schmidt (1965) model of galactic rotation. This procedure implies:

(1) That the kinematics of ionized and neutral hydrogen are identical.

(2) That the distance ambiguity of H II regions inside the solar circle can be resolved.

The first question has been investigated in three papers (Dieter, 1967; Kerr *et al.*, 1968; Mezger *et al.*, 1970) and an affirmative answer was obtained. The second problem, the distance ambiguity, can in principle be resolved from observations of the radio absorption spectrum of the interstellar matter between the source and the sun. To date, most of the relevant absorption measurements were made at 21 cm. It appears, however, that some of the molecular lines, e.g. those emitted by the OH- and $H_2CO$-molecules, may be better suited for this purpose since they are generally seen only in absorption.

Figure 6 shows the projected positions of all H II regions whose kinematic distances were obtained. Both 'near' and 'far' distances are given for those sources whose distance ambiguity could not be resolved. The resulting distribution is typical for similar investigations of the galactic structure: The source distribution exhibits a more or less radial structure, with the source density decreasing with increasing distance from the sun. Such a result should be anticipated, since we obviously observe the superposition of a local distribution of intrinsically weak H II regions and another distribution much more narrowly confined to the galactic plane which represents the distant 'giant' H II regions (see Section 4). It is this latter group of giant H II regions, however, which appears to outline the spiral structure in external galaxies (see, e.g., Hodge, 1969a). For an elimination of the local weak H II regions, we define a giant

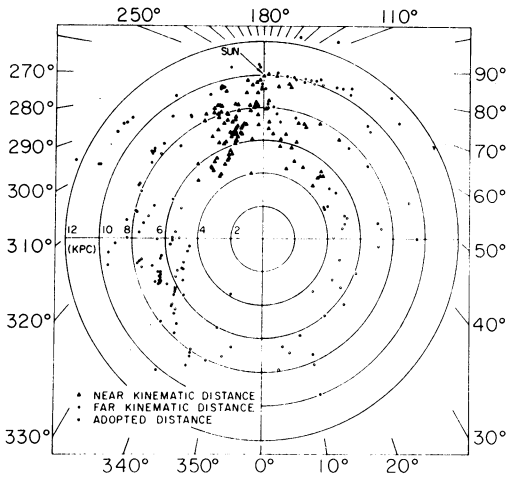


Fig. 6. Projected positions of HII regions whose H 109α emission was detected.

HII region somewhat arbitrarily by the condition

$$\left[\frac{S_5}{\text{f.u.}}\right]\left[\frac{D_{\text{near}}}{\text{kpc}}\right]^2 \geqslant 400$$

with $S_5$ the continuum flux density at 5 GHz and $D_{\text{near}}$ the 'near' kinematic distance of the source. In this way we eliminate all HII regions with flux densities less than four times the flux density of the Orion Nebula. The remaining distribution of giant HII regions is shown in Figure 7. The clustering of sources around the sun has disappeared but the general source density is still considerably higher on our side of the galactic center. This result is not unexpected since both H 109α surveys are complete for giant HII regions only out to distances of about 10 kpc from the sun. The minimum peak flux density of sources in any future recombination line survey has to be decreased by at least a factor of 4 if one wants to include all giant HII regions within the solar circle. It appears doubtful if this can be achieved with any radio telescope presently in operation.

## 6. Spiral Structure and Radial Distribution of HII Regions and Neutral Gas

We expect the spiral structure of our galaxy to be outlined by HII regions, especially by giant HII regions. The distribution of giant HII regions as derived from kinematic distances (Figure 7), however, does not reveal a clear-cut spiral structure. This may be partly due to instrumental selection effects. But one should be aware of the fact that giant HII regions in external galaxies in most cases do not outline a very clear-cut spiral pattern either (e.g. Hodge, 1969a). It appears that in most cases where photographs of external galaxies show a well-defined spiral pattern, this is the combined result of the presence of HII regions and the presence of luminous early-type

https://doi.org/10.1017/S0074180900000383 Published online by Cambridge University Press

stars (Hodge, private communication). Within the spiral arms, the giant H II regions very often exhibit a rather patchy distribution. We know that H II regions, especially those with a high surface brightness, must have rather short lifetimes, even if compared with the main sequence lifetime of OB-stars. It appears that giant H II regions are indicators of presently active regions of star formation, whereas OB-star associations and clusters represent those regions where star formation on a large scale happened during the past $10^6$ to $10^7$ years.

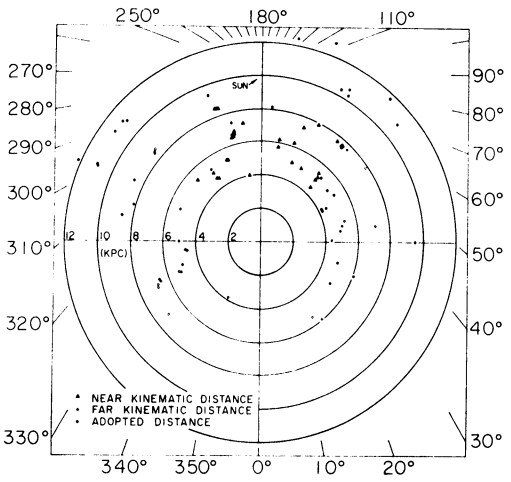


Fig. 7. Projected positions of giant H II regions only.

In Figure 7 one recognizes a ring of giant H II regions between roughly 4 and 6 kpc. There are similar but not as conspicuous concentrations of giant H II regions farther out from the galactic center which may outline parts of spiral arms, but there is no unambiguous way to connect these features in the northern and southern part of the galaxy. This is certainly in part a consequence of the fact that kinematic distances become highly unreliable at low galactic longitudes. Therefore, we may expect to get a more clear-cut picture by combining the local distribution of H II regions based on photometric distances (Courtès *et al.*, 1968, and Figure 2) with the distribution of giant H II regions (Figure 7). The result is shown in Figure 8. It is obvious that the high pitch angles obtained for the three pieces of spiral arms in the vicinity of the sun are incompatible with the large-scale spiral pattern as outlined by giant H II regions. However, I want to reiterate that we are dealing here with two different classes of objects, viz. optically observed, intrinsically weak H II regions on the one side and giant H II regions on the other, which indicate the birth of O-star associations but are primarily observable by their radio radiation.

What do we know about the radial distribution of H II regions in our galaxy? Hodge (1969b) has determined the radial distribution of giant H II regions* in a

* At present it is not possible to define the H II regions observed by Hodge in a quantitative way as we do for the radio 'giant' H II regions. We can only guess that this must be similar objects.

https://doi.org/10.1017/S0074180900000383 Published online by Cambridge University Press

number of external galaxies. Roberts (1968) found that the distribution of HII regions and neutral hydrogen in some external galaxies, which he investigated, are markedly different. The HII regions generally appear to be concentrated in an inner ring, the HI in an outer ring with the two rings scarcely overlapping. Westerhout, as early as 1958, suggested such a distribution of ionized and neutral gas in our own galaxy, but his interpretation was later questioned by Mathewson *et al.* (1962). With the present data we can investigate the radial distribution of HII regions in our own galaxy in a quantitative way. Figure 9a shows the number of giant HII regions in rings 1 kpc wide each. Only the five giant HII regions possibly located inside the 4 kpc arm are uniformly spread out in this graph between 0 and 4 kpc. The distance ambi-

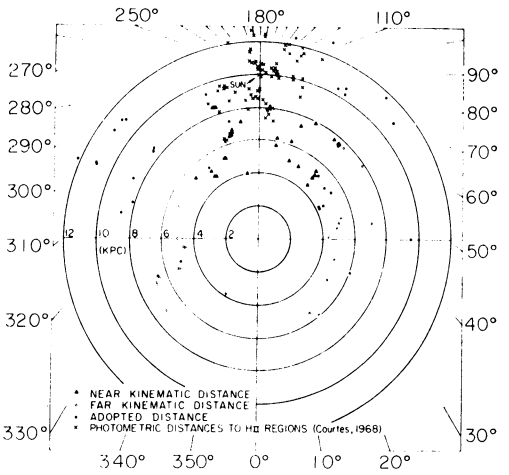


Fig. 8. Combination of projected positions of optically visible local HII regions (Figure 2) and giant HII regions (Figure 7).

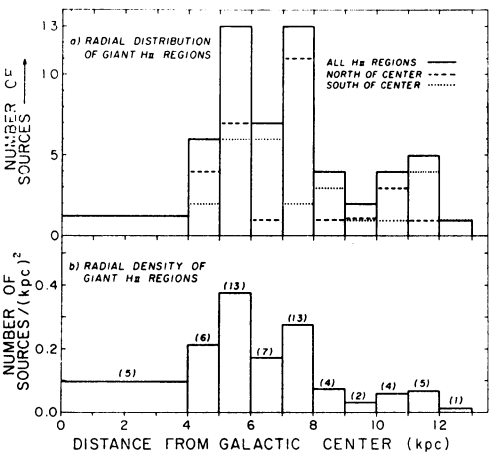


Fig. 9 (a)–(b). Radial distribution of giant HII regions.

https://doi.org/10.1017/S0074180900000383 Published online by Cambridge University Press

guity does not affect the radial position but only the azimuthal position of an H II region. As mentioned earlier, our radio survey of giant H II regions is complete out to a distance of 10 kpc only. Therefore, a more complete survey will certainly increase the number of giant H II regions and will also slightly alter the shape of the distribution function by giving more weight to the outer rings. In Figure 9b the corresponding source density is shown. There is a maximum between 5 and 6 kpc and a secondary maximum between 7 and 8 kpc. The most obvious feature in the distribution of giant H II regions is the broad maximum between 4 and 8 kpc and the virtual non-existence of giant H II regions outside 12 kpc.

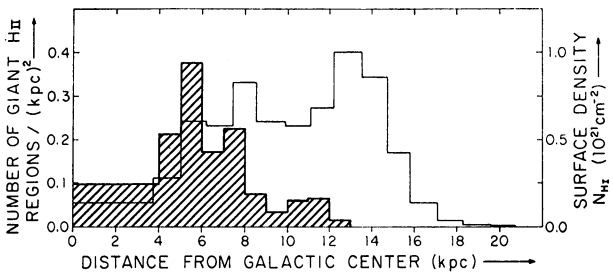


Fig. 10. Comparison of density of giant H II regions and surface density of neutral hydrogen as a function of the distance from the galactic center.

In Figure 10 the density distribution of giant H II regions (Figure 9b) is compared with the radial distribution of the surface density of neutral hydrogen as recently derived by Van Woerden (Oort, 1965). The latter distribution attains its maximum value at about a distance of 13 kpc from the galactic center, where no giant H II regions are observed. It thus appears that a high density of neutral hydrogen is a necessary but not a sufficient condition for the formation of O-star clusters and associations and that other physical parameters – such as e.g. Lin's density wave – play an important role in this process, too.

It should be mentioned here, at least, that the two H 109$\alpha$ surveys of the northern and southern sky reveal some basic differences. We are still investigating selection effects which are certainly introduced by the two different radio telescopes used in these surveys. It is only after these instrumental effects have been sorted out that we can try to interpret a possible genuine difference in the northern and southern distributions.

## Acknowledgements

It is a pleasure to thank W. Altenhoff and T. L. Wilson for their help in preparing this review paper. I want further to thank P. W. Hodge and Miss E. Sim for helpful comments.

## References

Altenhoff, W.: 1968, in *Interstellar Ionized Hydrogen* (ed. by Y. Terzian), Benjamin, New York, p. 519.
Altenhoff, W., Mezger, P. G., Wendker, H., and Westerhout, G.: 1960, *Veröff. Univ. Sternwarte Bonn* **59**, 48.
Altenhoff, W., Downes, D., Goad, L., Maxwell, A., and Rinehart, R.: 1969, in press.
Blaauw, A.: 1964, *Ann. Rev. Astron. Astrophys.* **2**, 213.
Churchwell, E. and Felli, M.: 1969, several papers, in preparation.
Clark, B. G.: 1965, *Astrophys. J.* **142**, 1398.
Courtès, G., Georgelin, Y., Monnet, G., and Pourcelot, A.: 1968, in *Interstellar Ionized Hydrogen* (ed. by Y. Terzian), Benjamin, New York, p. 571.
CSIRO: 1969, in preparation.
Dieter, N. H.: 1967, *Astrophys. J.* **150**, 435.
Felli, M. and Churchwell, E.: 1969, in preparation.
Goss, W. M. and Shaver, P. A.: 1969, in preparation.
Hill, E. R.: 1968, *Australian. J. Phys.* **21**, 735.
Hodge, P. W.: 1969a, *Astrophys. J. Suppl. Ser.* **18**, 73.
Hodge, P. W.: 1969b, *Astrophys. J.* **155**, 417.
Höglund, B. and Mezger, P. G.: 1965, *Science* **150**, 339.
Kerr, F. J., Burke, B. F., Reifenstein, E. C., Wilson, T. L., and Mezger, P. G.: 1968, *Nature* **220**, 1210.
Lin, C. C. and Shu, F. H.: 1964, *Astrophys. J.* **140**, 646.
Lin, C. C. and Shu, F. H.: 1966, *Proc. Nat. Acad. Sci. Am.* **55**, 229.
Mathewson, D. S., Healey, J. R., and Rome, J. M.: 1962, *Australian. J. Phys.* **15**, 354, 369.
McGee, R. X. and Gardner, F. F.: 1968, *Australian. J. Phys.* **21**, 149.
Mebold, U.: 1969, *Beiträge zur Radioastronomie* **1**, 97.
Mezger, P. G.: 1969, *Colloque Internat. Liège No. 16*, in press.
Mezger, P. G. and Henderson, A. P.: 1967, *Astrophys. J.* **147**, 471.
Mezger, P. G. and Höglund, B.: 1967, *Astrophys. J.* **147**, 490.
Mezger, P. G., Wilson, T. L., Gardner, F. F., and Milne, D. K.: 1970, *Astron. Astrophys.* **4**, 96.
Oort, J. H.: 1965, *Trans. IAU* **12A**, 789.
Reifenstein, E. C., Wilson, T. L., Burke, B. F., Mezger, P. G., and Altenhoff, W. J.: 1970, *Astron. Astrophys.* **4**, 357.
Roberts, M. S.: 1968, in *Interstellar Ionized Hydrogen* (ed. by Y. Terzian), Benjamin, New York, p. 617.
Schmidt, M.: 1965, *Stars and Stellar Systems* **5**, 513.
Schraml, J. and Mezger, P. G.: 1969, *Astrophys. J.* **156**, 269.
Sharpless, S.: 1959, *Astrophys. J. Suppl. Ser.* **4**, 257.
Shaver, P. A. and Goss, W. M.: 1969, in preparation.
Sim, M. E.: 1968, *The Royal Observatory, Edinburgh, Publ.* **6**, No. 5.
Westerhout, G.: 1958, *Bull. Astron. Inst. Netherl.* **14**, 215.
Wilson, T. L., Mezger, P. G., Gardner, F. F., and Milne, D. K.: 1970, in preparation.

## Discussion

*Van Woerden:* The neutral-hydrogen surface densities quoted by Mezger have been derived by me from Westerhout's (1957, *Bull. Astron. Inst. Netherl.* **13**, 201) 'cross-sections' at constant $l^{II}$, by integrating hydrogen densities along lines perpendicular to the plane and then averaging the resulting surface densities in concentric rings around the center. In comparing these HI surface densities with the numbers of HII regions, one should bear in mind that the effective layer thickness of HI increases outward; the radial distribution of HI volume density differs less from that of HII regions than does the distribution of surface density.